Representation of the Strain Histories in a Cup Drawing

Takaji MIZUNO and Kenji KAKEDA

Department of Mechanical Engineering
(Received September 13, 1971)

Since the principal directions of the strains are fixed with respect to the work material in the axisymmetrical cup drawing process, the strain distributions and the strain histories may be represented by the strain paths on the deviatoric strain plane. This paper shows that a set of strain paths on the deviatoric plane, practically drawn on a triangular coordinate graph paper, can facilitate not only to realize the simultaneous development of the three principal strains but also to infer the progress of the stress state during the process.

1. Introduction

An important feature of deep-drawing process is that the required tensile force to draw in the flange part must be transmitted through the cup wall and the stretch-forming region from the punch head. The deep-drawing capacity, therefore, can be increased only if the strength of the cup wall can be increased relatively to the required drawing load.

For a relatively thick sheet metal which needs no blank-holding pressure to prevent wrinkling of the flange during radial drawing, the punch load can be reduced by using a conical die[1] or a tractrix die which minimize the redundant work due to the friction on die surface and the plastic bending and unbending on die profile. Hence, a larger limiting drawing ratio (L. D. R.) can be attained than when using a flat die. Here, it should be also noted that the strength of the cup wall can be slightly increased as an additional effect of reducing the punch load.

The strength of the cup wall or of the stretch-forming region is influenced in a complicated manner by a number of process variables, such as punch profile radius, lubrication of punch, work-hardening characteristics and normal anisotropy of material, die profile radius, drawing ratio and so on. Furthermore, in the mathematical analysis of the stretch-deformation it is necessary to use the drawing load in every stage of the process as a boundary condition. The results of many investigations, however, show that there can be an optimum combination of punch profile radius, friction and work-hardening characteistics of material for increasing the strength of the cup wall[2),3)].

Concerning the material properties, it has been recognized that there is direct correlation between deep-drawability and the "r" value or width-strain to thickness-strain ratio obtained from a tensile test which represents the normal anisotropy of the blank material[4)]. Because a material with a larger "r" value shows higher resistance to stretch-deformation and, on the other hand, lower resistance to radial drawing than an isotropic material with "r" value of unity. Simplified mathematical analyses also revealed that L. D. R. depends on "r" value more markedly than the work-hardening index"n"[5),6),7)]. However, it seems that deep-

drawability can not completely be determined by only the "r" value, because it is also influenced by many other process variables.

Complete assesment of deep-drawability requires complete assesment of the strength of the cup wall, in other word, of the tension transmitting capacity of the stretch-forming region. It can be said that the strength is a function of both the material characteristics and the strain history which the material follows, though the analytical treatment is not easy. It seems necessary, therefore, to investigate the strain histories in cup drawing in detail.

The strain history has been expressed partly by the development of the distribution of one principal strain i.e. through-thickness strain since H. W. Swift[8]. Recently, K. Yoshida[9] has drawn the strain paths in the Cartesian plane coordinates using two strains measured in the plane of the sheet. Such a figure is called 'deformation diagram' or 'strain composition diagram' and has been extensively applied for investigating the press formability, especially of autobody parts, together with scribed circles method.

However, if the directions of principal strains remain fixed with respect to the material as in drawing a round cup from isotropic blank, there exists a more complete and fundamental method of representation of the strain histories. That is, a strain state can be indicated properly by a vector which lies on the deviatoric strain plane in the Cartesian coordinates space and the strain history by the strain path i.e. the locus generated by the vector. And, a strain path on the deviatoric strain plane can be related to a stress path on the deviatoric stress plane π. Examining the strain paths on the deviatoric strain plane, therefore, one can not only realize the distributions of the three principal strains at a time and the simultaneous development of the three strains, but also infer the development of the stress state during the process.

In the present paper, the fundamentals of the method above mentioned are shown, and it is demonstrated how clearly the deformation behavior of the material during cup drawing can be indicated by the strain paths on the deviatoric plane.

2. Geometry on the Deviatoric Strain Plane

If the principal directions remain constant during deformation, the state of plastic strain at a point in the work material can be described in Cartesian space coordinates by a point Q, the coordinates of which are the values of the principal strains $\varepsilon_1, \varepsilon_2, \varepsilon_3$. Such a strain point Q lies on the deviatoric plane described by the equation $\varepsilon_1+\varepsilon_2+\varepsilon_3=0$, inclined by the same angle in relation to each of the coordinate axes, because there is no permanent change in volume. The representaion in space can be reduced to that in plane by projecting the point Q and the coordinate axes on the deviatoric plane $\varepsilon_1+\varepsilon_2+\varepsilon_3=0$. Thus a plane system of three coordinate axes concurring in origin, the angles between the neighbouring axes being 120°, is obtained as shown in Fig. 1 (a). The actual lengths of the vectors OS, ST, and TQ, representing ε_1, ε_2, and ε_3 in space respectively, are projected on the plane as $\sqrt{2/3}\cdot\varepsilon_1$, etc.. And the components OS, ST, TQ can be found from the strain point Q by the relations $OS=2/3\cdot OQ_1$, $ST=2/3\cdot OQ_2$, $TQ=2/3\cdot OQ_3$ analogous to the well known Hill's construction in the deviatoric stress plane, where QQ_1, QQ_2, QQ_3 are the perpendiculars dropped on the projected axes from Q. Thus OQ_1, OQ_2, OQ_3 represents $\sqrt{3/2}\cdot\varepsilon_1$, etc., and the length of the vector $OQ=\sqrt{\varepsilon_1^2+\varepsilon_2^2+\varepsilon_3^2}=\sqrt{3/2}\cdot\bar{\varepsilon}$ where $\bar{\varepsilon}$ is the

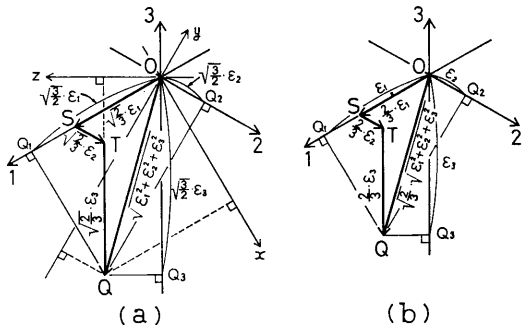

Fig. 1 Geometry in deviatoric plane

epuivalent total strain.

It is more convenient to multiply the vector projections on the deviatoric plane by $\sqrt{2/3}$, as shown in Fig. 1 (b). OQ becomes equal to the equivalent total strain $\bar{\varepsilon}$, and OQ_1, OQ_2, OQ_3 represents $\varepsilon_1, \varepsilon_2, \varepsilon_3$ respectively. The relations facilitate to plot the strain point and to draw the strain path on a triangular coodinate graph paper, and to read the three principal strains from a point on the strain path.

3. Experimental Procedure

The deep drawing operations were performed in a hydraulically operated cup drawing tester with a capacity of 12 tons. The dimensions of the tools are as shown in Table 1. The work materials are aluminum and "Drawability" steel of 1mm thickness. The mechanical properties are as shown in Table 2.

Table 1 Dimensions of punch and die

Punch diameter	40.0mm
Punch profile radius	8.0mm
Die hole diameter	43.0mm
Die profile radius	8.0mm

Table 2 Mechanical properties of material

Material	Proof stress (kg/mm²)	Tensile strength (kg/mm²)	Uniform elongation	"r" value	L.D.R.
Aluminum-0	2.9	9.2	0.27	0.80	2.16
Aluminum-1/2H	11.4	11.5	0.07	1.07	2.13
"Drawability" steel	15.6	30.9	0.24	1.60	2.31

Note : The values are those averaged as fllows; $(\ ) = 1/4\{(\ )_0 + 2(\ )_{45} + (\ )_{90}\}$

In this study, both the punch and die were lubricated with Grephite-H (graphite in tallow), and constant blank-holding forces of 200kg, 350kg and 900kg were applied for aluminum-0, aluminum-1/2H and "Drawability" steel respectively. And the drawing speed was kept constant approxmately 5mm/min.. The limiting drawing ratios obtained under these conditions are also shown in Table 2. The strain histories in cup drawing were investigated with 83.0mm dia. blanks (the corresponding drawing ration is 2.075), and the drawing process was stopped at seven

different punch travels, including the fully drawn cup, with one specimen for each.

For measuring the strains in the work material, concentric circles and radial lines intersecting to the rolling direction at 0, 45 and 90 degree were scribed on the die-side surface of the blank. The through-thickness strain ε_t was determined as follows:

$$\varepsilon_t = \log_e (t/t_0) \quad \cdots\cdots (1)$$

Where t_0 is the initial thickness of the blank and t the current thickness. However, since the strains distribute approximately linearly in the through-thickness direction at the curved parts of the cup, except for the flat bottom and the flat flange, ε_t thus determined is one on the centre surface between the two surfaces of the work. Therefore, the corresponding circumferential strain ε_θ should be determined also on the same centre surface as follows:

$$\varepsilon_\theta = \log_e (d/d_0) \quad \cdots\cdots (2)$$

Where d_0 is the initial diameter of ascribed circle and d the current diameter on the centre surface determined by taking the thickness and the direction of the current normal to the surface into consideration.

The third principal strain ε_ϕ was determined by using the following equation.

$$\varepsilon_\phi = -(\varepsilon_t + \varepsilon_\theta) \quad \cdots\cdots (3)$$

4. Experimental Results

4.1 Strain Distributions and Strain Histories

Figure 2 shows a typical example of the strain distributions and the strain histories represented in the triangular coordinate system. The work material is aluminum-0 which exhibits negligible earing, and the blank diameter is 83.0mm.

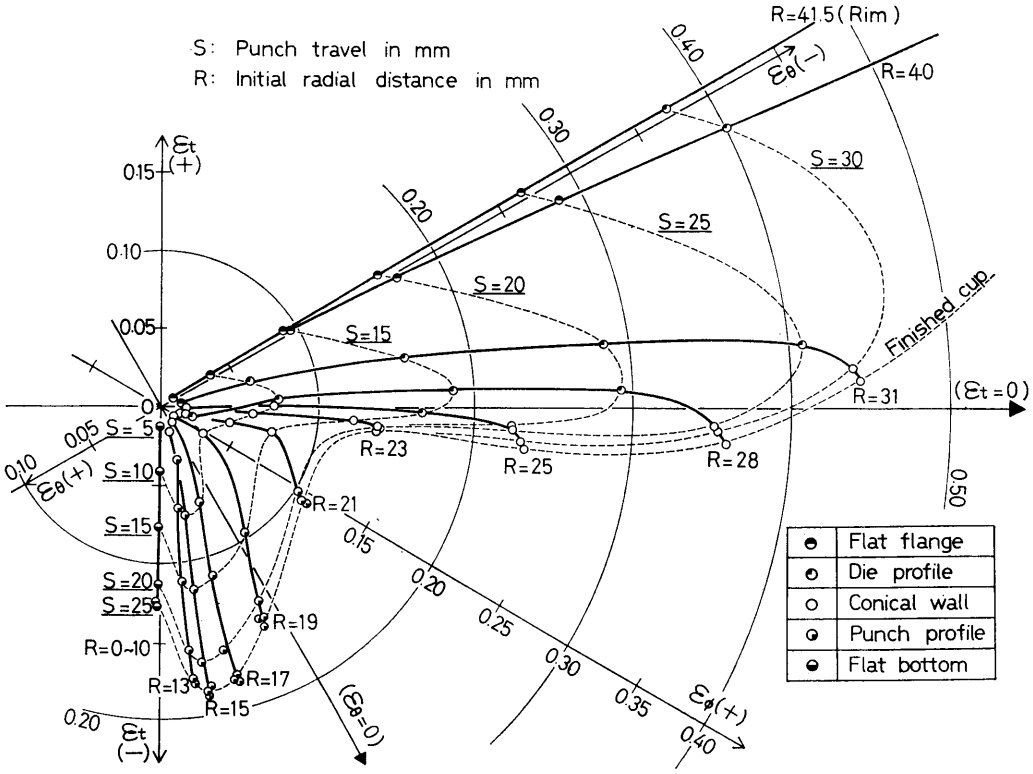

Fig. 2 Strain paths in cup drawing of aluminum-0

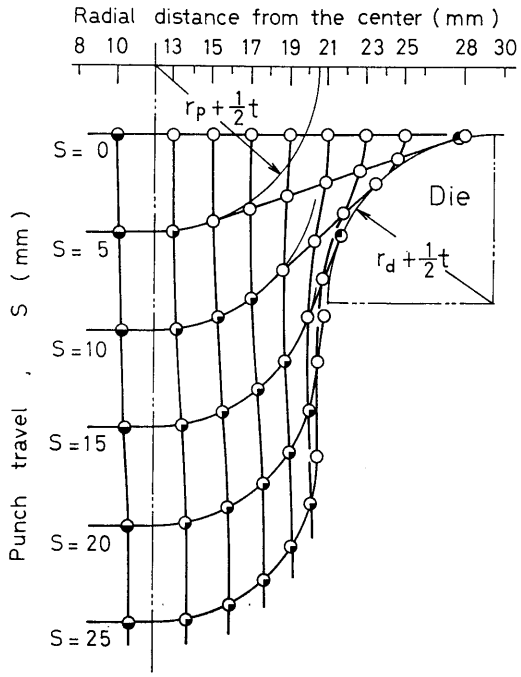

Fig. 3 progressive change in position of the materials in stretch-forming region

At the flat bottom of the punch, the material (the initial radial distance from the centre of the blank; R=0～10mm) is stretched in biaxial tension, producing uniform thinning, hence the strain path is along the negative ε_t axis ($\varepsilon_t=-2\varepsilon_\theta=-2\varepsilon_\phi$). On the other hand, the material undergoes an almost pure compression in the circumferential directon at the rim (R=41.5mm in this case), hence the strain path is expected to be along the negative ε_θ axis for an isotropic material, However, since the aluminum-0 has a "r" value of 0.80, the strain path deviates from the negative ε_θ axis by just a short distance towords the positive ε_t axis.

Noticing the behavior of the material which contacts with the punch profile, it is seen from Fig. 2 that on coming contact with the punch profile the material is subjected to an additional strain of remarkable magnitude by the plastic bending under tension. (In the figure, ○ means that the material touches neither die nor punch, and ◔ indicates the material being on the punch profile.) As seen from Fig. 3 which shows the change in position of the material in the stretch-forming region, the material at R=13mm comes in contact with the punch profile when the punch travel S=0～5mm, the material at R=15 & 17mm when S=5～10mm, the material at R=19mm when S=10～15mm, and the material at R=21mm when S=15～20mm.

It should be also noted that when the material touches the punch profile and undergoes bending, the strain path tends to turn its direction perpendicular to ε_θ axis, in other word, the deformation due to the additional bending uder tension is nearly plane strain in $t\phi$-plane, and that after coming contact with the punch profile, the material is stretched in nearly balanced biaxial tension in this case where the punch is lubricated.

On the other hand, a thinning due to the plastic bending on the die profile is observed only for the material at R=28mm in the early stage. The thinning is,

however, offset by the subsequent thickening due to radial drawing. On leaving the die profile, the material undergoes plastic unbending under tension. This effect is clearly observed in Fig. 2 for the material at R=25~31mm. Again, it is pointed out that the deformation due to the unbending under tension is plane strain in $t\phi$-plane.

Between the fibres associated with bending and unbending over the die profile and with bending and stretching over the punch profile, there is a narrow band which escapes plastic bending throughout the process. As seen from Fig. 2 and Fig. 3, such a fibre exists at R=23mm in this case and thins a less extent than the fibres on either side. The strain path is a straight radial and nearly perpendicular to ε_t axis representing proportional and nearly plane strain deformation in which $d\varepsilon_t=0$.

4.2 Evaluation of Stress Distribution in Stretch-Forming Region

The influence of plastic bending under tension is manifested in Fig. 4 in which the three strains are plotted against the distance along the meridional contour. ε_ϕ and ε_t change discontinuously at both ends of the punch profile. The corresponding stress distributions in this stage can be evaluated from the strain paths shown in Fig. 2.

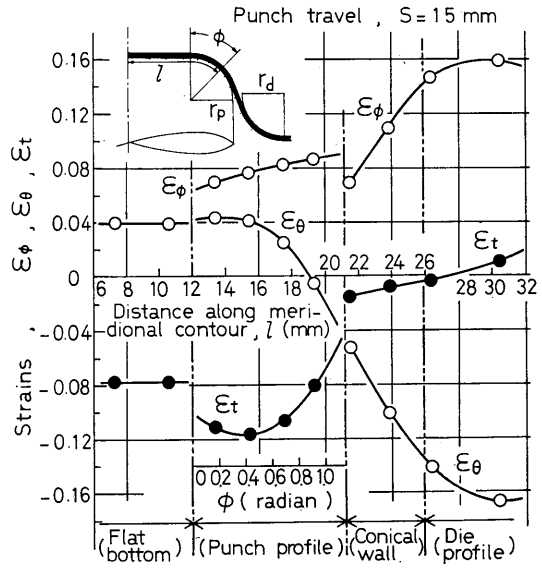

Fig. 4 Strain distribution in the stretch-forming region

If it can be assumed that the material exhibits only normal anisotropy, the stress-strain increment relation yields

$$\xi=\frac{d\varepsilon_\theta}{d\varepsilon_\phi}=\frac{(\sigma_\theta-\sigma_\phi)+(\sigma_\theta-\sigma_t)/\bar{r}}{(\sigma_\phi-\sigma_\theta)+(\sigma_\phi-\sigma_t)/\bar{r}} \quad \cdots\cdots(4)$$

where, ξ: ratio of the circumferential strain increment $d\varepsilon_\theta$ to the meridional strain increment $d\varepsilon_\phi$ which is determined from the strain path in Fig. 2

σ_θ: circumferential stress

σ_ϕ: meridional stress

σ_t: through-thickness stress, which may be assumed to be $-1/2\cdot p$, where p is pressure on the punch profile

$\bar{r}$: mean "r" value of the material

Equilibrium in through-thickness direction can be written

$$p/t=\sigma_\theta\cdot\sin\phi/r+\sigma_\phi/r_p \quad\cdots\cdots(5)$$

where, p: pressure on the inside surface of the material

t: thickness of the material

ϕ: angle measured from the vertical line as shown in the inset of Eig. 4

r: radial distance from the centre

r_p: radius of the punch profile

Equivalent stress $\bar{\sigma}$ for the material with only normal directionality can be written

$$\bar{\sigma}=\sqrt{\frac{3}{2(\bar{r}+2)}}\cdot\sqrt{\bar{r}(\sigma_\phi-\sigma_\theta)^2+(\sigma_\theta-\sigma_t)^2+(\sigma_t-\sigma_\phi)^2} \quad\cdots\cdots(6)$$

$\bar{\sigma}$ is evaluated from the equivalent stress-strain diagram reduced from the tensile test and the equivalent strain $\bar{\varepsilon}$ which the material suffered in cup drawing. If the material is isotropic, $\bar{\varepsilon}$ is given by the length of a particular strain path. However, since the equivalent strain for the assumed material with normal directionality is defined as follows;

$$\bar{\varepsilon}=\sqrt{\frac{2(2+\bar{r})}{3(1+2\bar{r})^2}}\cdot\int\sqrt{\bar{r}(d\varepsilon_\phi-d\varepsilon_\theta)^2+(d\varepsilon_\theta-\bar{r}d\varepsilon_t)^2+(\bar{r}d\varepsilon_t-d\varepsilon_\phi)^2} \quad\cdots\cdots(7)$$

$\bar{\varepsilon}$ was determined in this study by approximating a curved strain path by a broken line composed of two or three straight segments having constant strain ratios ξ.

The calculated stress distributions are as shown in Fig. 5, including the results for isotropic material. Over the flat bottom, $\sigma_\phi=\sigma_\theta$ and they are uniformly distributed. This corresponds to the uniform distribution of the strains and suggests no interfacial pressure between the flat bottom of the punch and the material. σ_ϕ changes discontinuously at $\phi=0$ corresponding the discontinuous change in ε_ϕ, and has a maximum on the punch profile. The estimated pressure distribution was fairly uniform over the punch profile, and the integration of the pressure over the punch profile area gave a punch load of 805kg for the measured load of 840kg.

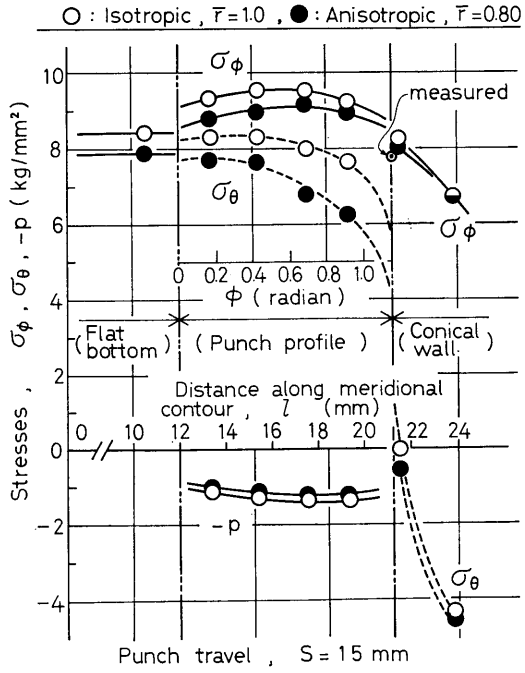

Fig. 5 Calculated stress distribution in the stretch- forming region

At the another end of the contact arc (at $\phi=1.17$ radian in this case), σ_ϕ changed rather moderately but σ_θ changed abruptly from positive to negative. In consequence, it can be seen that the material, just before coming contact with the punch profile, suffers uniaxial tension in the meridional direction, and the material which stays in the conical wall throughout the process suffers nearly pure shear ($\sigma_\phi \fallingdotseq -\sigma_\theta$) as shown also in Fig. 2.

Figure 6 shows the distribution of the tension per unit width $t\sigma_\phi$. The gradients $d(t\sigma_\phi)/dr$ were constant over the punch profile; 0.10kg/mm^2 for the punch travel S=10mm and 0.09kg/mm$_2$ for S=15 & 20mm. Coefficients of friction μ on the punch profile were estimated by substituting these values into the equilibrium equation (8) in radial direction.

$$\frac{d(t\sigma_\phi)}{dr}=\frac{t(\sigma_\theta-\sigma_\phi)}{r}+\frac{\mu p}{\cos\phi} \quad \cdots\cdots(8)$$

The results are as shown in Fig. 7. It seems that μ is not constant over the punch profile, but is not affected by punch travel.

4.3 Strain Paths of Different Work Materials

The strain paths of "Drawability" steel are shown in Fig. 8. Since this material

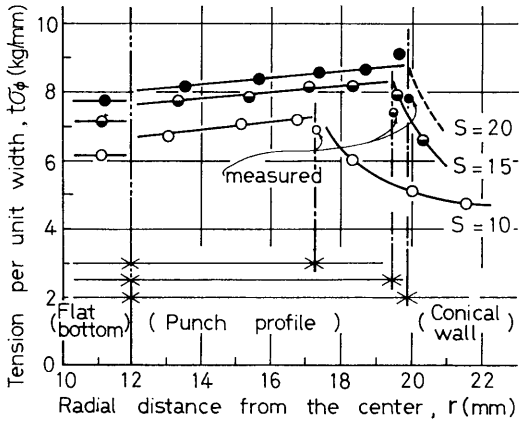

Fig. 6 Distribution of tension per unit width

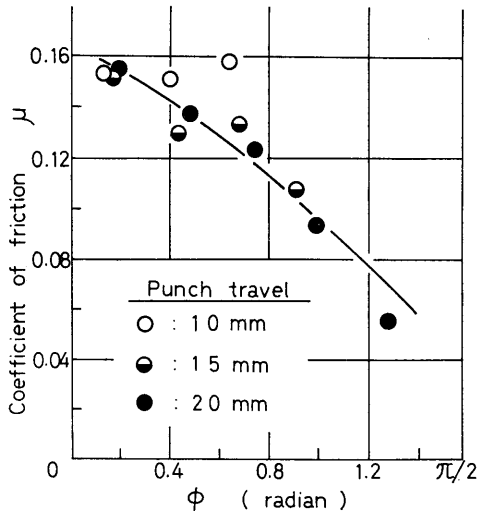

Fig. 7 Distribution of coefficient of friction on the punch profile

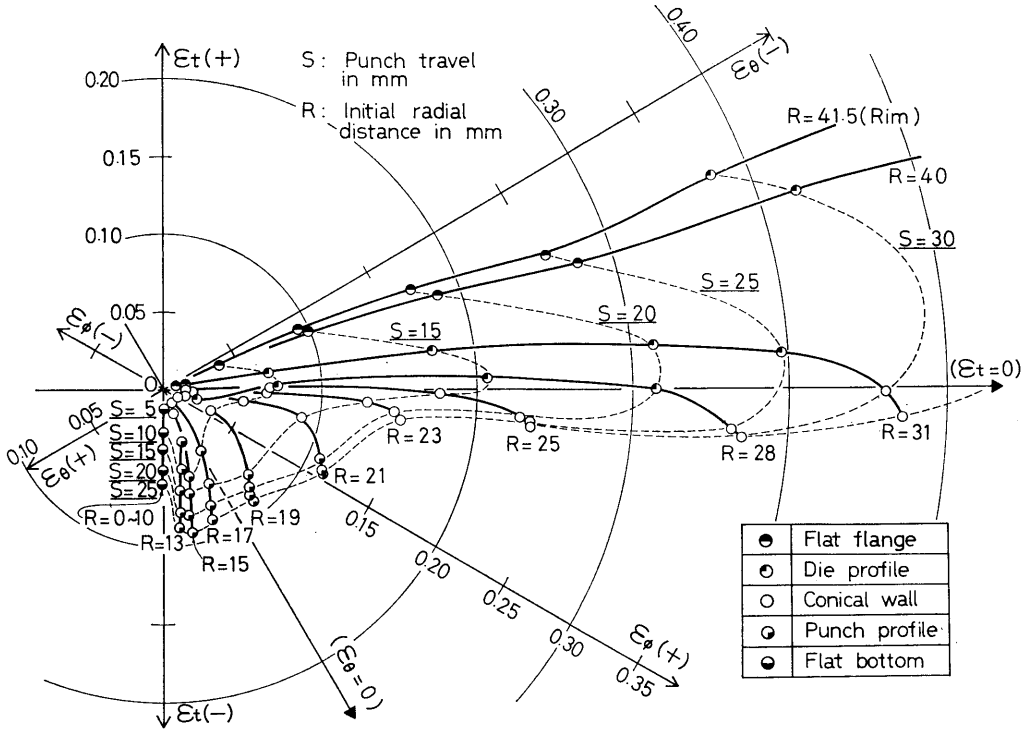

Fig. 8 Strain paths in cup drawing of "Drawability" steel

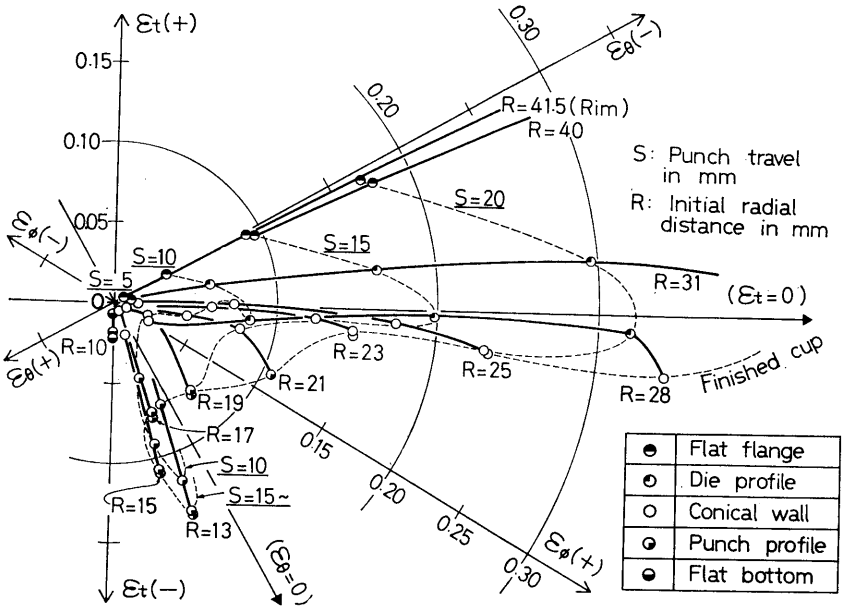

Fig. 9 oStrain paths in cup drawing of aluminum—1/2 H

has a large "r" value of 1.6, the strain path of the rim (R=41.5mm) deviates remarkably from the negative ε_θ axis towards the positive ε_ϕ axis, i.e., the thickening of the flange is less than aluminum-0. On the other hand, the thinning in the stretch-forming region occurs to a less extent than aluminum-0. As being broadly recognized, these two effects caused by the large "r" value bring the good

drawability of this material (Table 2). Remarkable increase in strain due to bending under tension, however, is observed in this material as in other materials.

Figure 9 shows the strain paths of aluminum-1/2 H. Since this material has a small strain hardening index of 0.09, the punch load increased at a higher rate in the early stage than the other two materials and reached a maximum when S=18 mm. The corresponding tension transmitted through the conical wall was estimated to have reached a maximum when S=15mm. In fact, the deformation in the stretch-forming region had ceased at S=15mm as seen in Fig. 9.

It is noticed that the increase in strains due to bending under tension is larger than in the other materials, producing a neck at R=13mm in the earlier stage. Since the strain at the flat bottom is little and the corresponding radial displacement is also little, the deformation of R=13mm approximates inevitably plane strain ($d\varepsilon_\theta$=0). As the result, the strain path of R=13mm deviated from the negative ε_t axis farther than even those of the outer fibres at R=15 & 17mm. The equivalent strain in the neck at R=13mm exceeded the uniform elongation of about 10% in the tensile test. Nevertheless, the process was successfully performed, probably because growing of the neck at R=13mm to fracture required a further deformation of the outer fibres at R=15~21mm, and the latter deformation required a slightly larger punch load.

5. Conclusion

It was demonstrated that the deformation behavior of the material in cup drawing can be fully visualized by the strain paths in the deviatoric strain plane, practically drawn on a triangular coordinate graph paper. One can find easily the simultaneous development of all the three strains, i.e. the strain history, from a strain path, also realize at a time the distributions of all the three strains in every stage from a set of strain paths being intersected by the consant punch travel lines. Furthermore, applying the incremental strain theory to such a strain analysis, one can also infer progress of the stress state during the process. Thus, it may be possible to examine the theories of deep drawing developed by this time. And, concerning actual problems, it may be possible that the drawabilities of different materials are discriminated on the basis of the strain paths.

References

1) Y. Kasuga and N. Tamakoshi : J. Japan Soc. Mech. Engrs., 62—489 (1959—10), 1430
2) Y. Kasuga : Press-Working, Kyoritsu Publications, Tokyo, 1965
3) N. Kawai et al. : Trans. Japan Soc. Mech. Engrs., 36—284 (1970—4), 681
4) W. T. Lankford, S. C. Snyder and J.A. Bauscher : Trans. A. S. M., 42 (1950), 1197
5) R. L. Whiteley : A. S. M., 52 (1960), 154
6) M. Fukuda : J. Japan Soc. for Technology of Plasticity, 5—36 (1964—1), 3
7) Y. Yamada : ibid., 5—38 (1964—3), 183
8) S. Y. Chung and H.W. Swift : Proc. Insth. Mech Engrs., 165 (1951), 199
9) K. Yoshida J. Japan Soc. Mech. Engrs., 73—614 (1970—3), 417